Supplementary Information:

Accelerating the generation and discovery of high-performance donor materials for organic solar cells by deep learning

*Jinyu Sun, Dongxu Li, Yue Wang, Ting Xie, Yingping Zou, Hongmei Lu *and Zhimin Zhang **

College of Chemistry and Chemical Engineering, Central South University, Changsha 410083, China

** Corresponding author E-mail: hongmeilu@csu.edu.cn;zmzhang@csu.edu.cn*

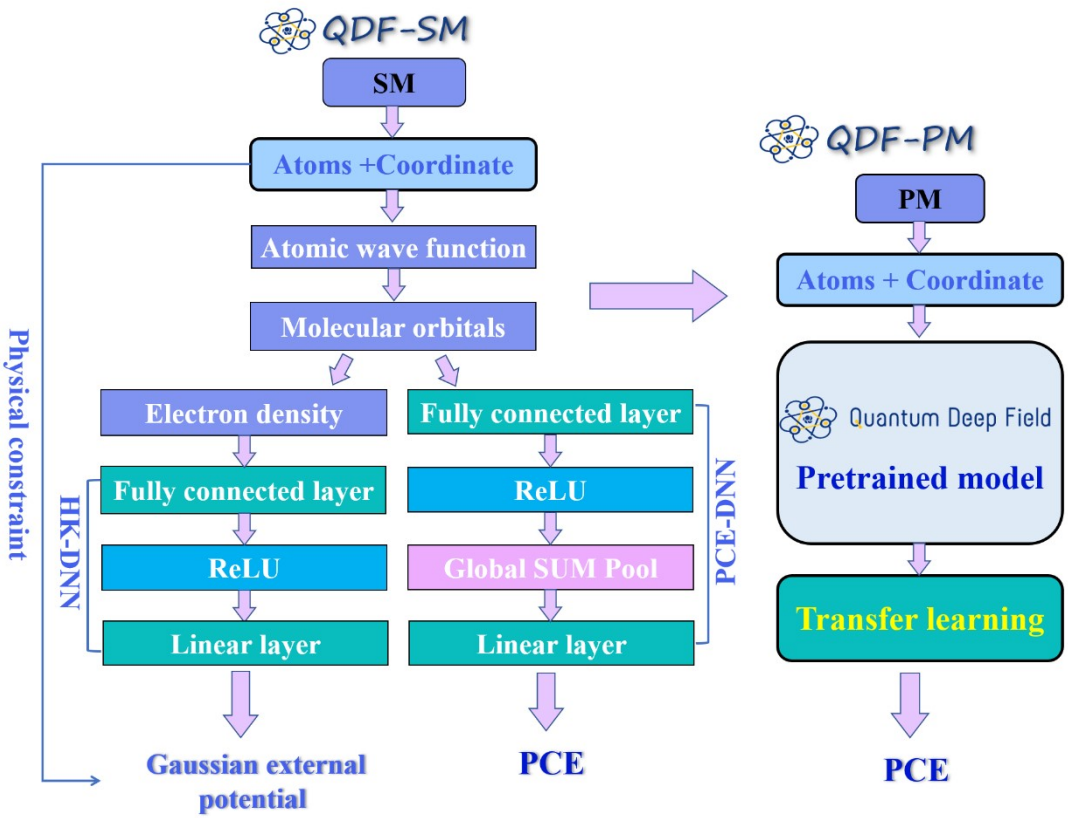

Figure S1. The architecture of quantum deep field in DeepDonor.

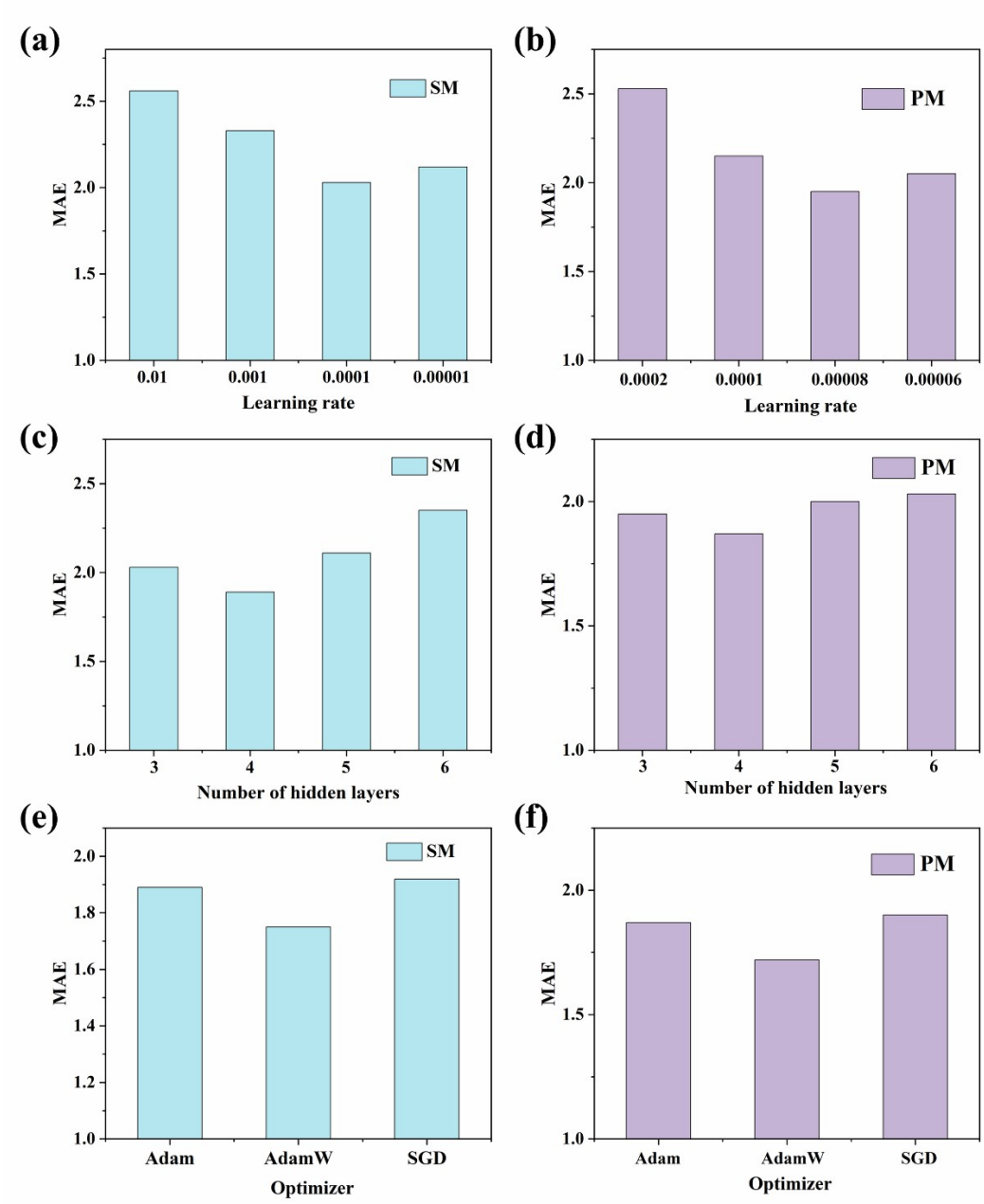

Figure S2. The results of hyperparameter optimization on the validation set. The selection of learning rate on the SM (a) and PM (b) datasets. The selection of numbers of hidden layers on the SM (c) and PM (d) datasets. The selection of optimizers on the SM (e) and PM (f) datasets.

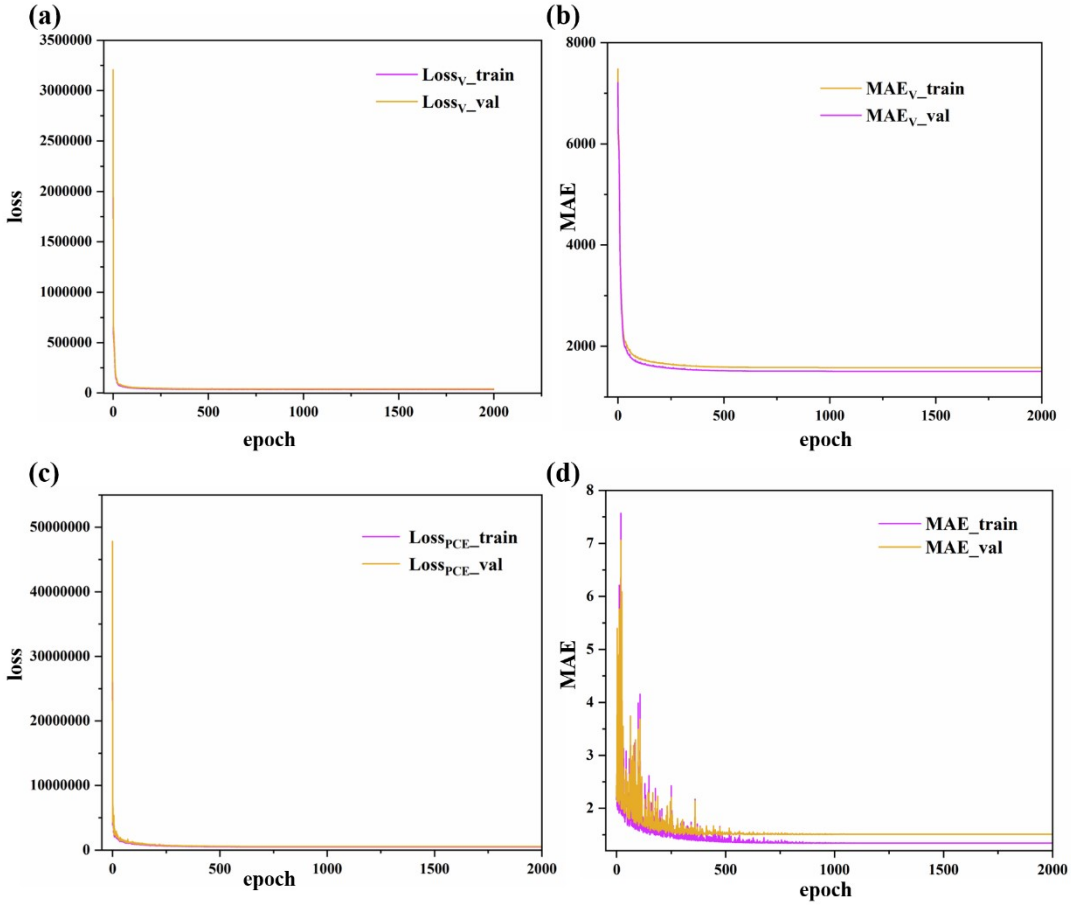

Figure S3. The learning curves of QDF-SM. The loss (a) and MAE (b) curves of HK-DNN of QDF-SM. The loss (c) and MAE (d) curves of PCE-DNN of QDF-SM.

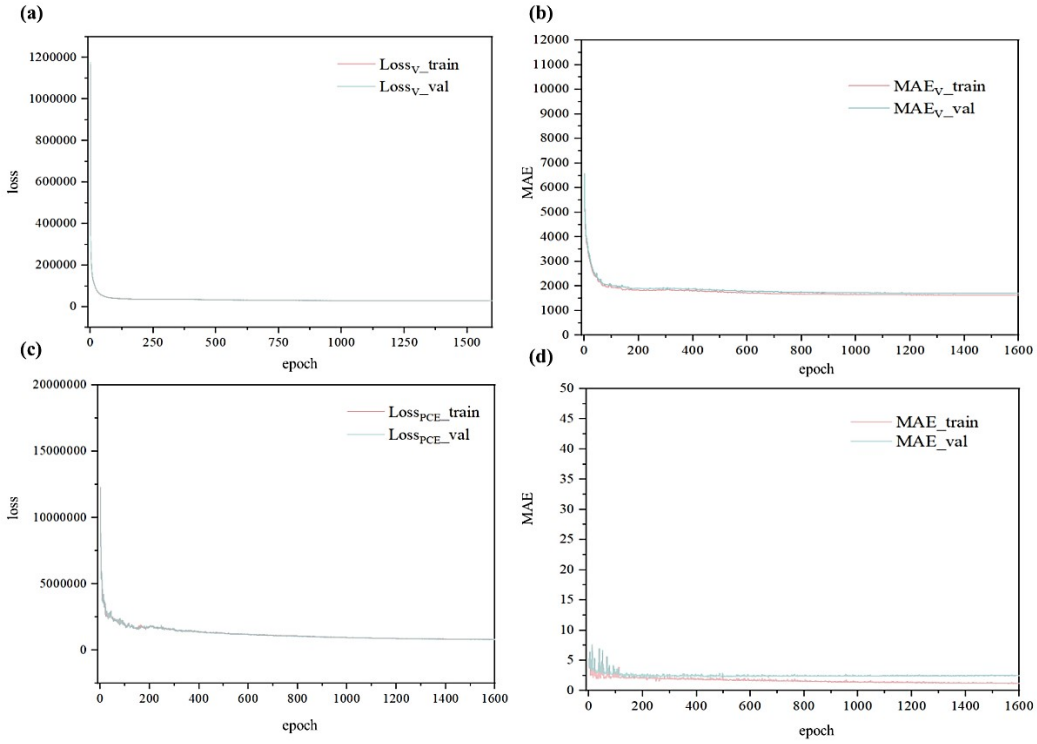

Figure S4. The learning curves of QDF-PM. The loss (a) and MAE (b) curves of HK-DNN of QDF-PM. The loss (c) and MAE (d) curves of PCE-DNN of QDF-PM.

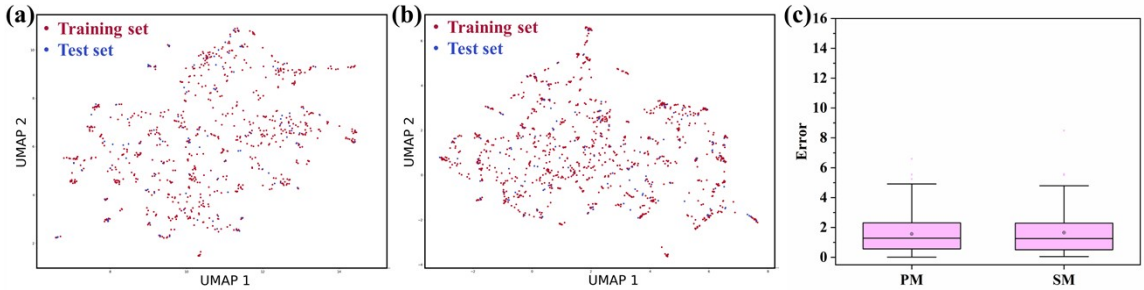

Figure S5. The UMAP low dimensional embedding of the training and test sets of SM (a) and PM (b) datasets. (c) The absolute error distribution of the test sets.

Table S1. Descriptors used for screening donor materials.

Descriptor	Description	Values
MolLogP	Wildman-Crippen LogP value	8.7~40.7
MolWt	The average molecular weight of the molecule	485~1967
NOCount	The number of Nitrogens and Oxygens	0~6
NumHAcceptors	The number of Hydrogen Bond Acceptors	3~15
NumHDonors	The number of Hydrogen Bond Donors	0~2
NumHeteroatoms	The number of Heteroatoms	5~18
NumRotatableBonds	The number of Rotatable Bonds	13~55
RingCount	Ring count	2~13
NumAromaticHeterocycles	The number of aromatic heterocycles	0~11
NumAromaticRings	The number of aromatic rings for a molecule	0~12
SAscore	Synthetic accessibility	0~7.5
SCScore	Synthetic complexity	<4.999
DeepChemStable	Compound stability	0~0.98
DeepDonor	PCE	>9

Table S2. Prediction results of different methods on the test sets

Data	Model	*r*	R^2	MAE	Accuracy
Small Molecule	DeepDonor	0.82	0.65	1.67	0.70
	GNN	0.66	0.61	2.05	0.59
	ANN	0.63	0.37	2.20	0.57
	RF	0.76	0.58	1.81	0.69
	GB	0.64	0.40	2.27	0.56
Polymer Molecule	DeepDonor	0.77	0.59	1.59	0.73
	GNN	0.71	0.42	1.70	0.71
	ANN	0.48	0.11	2.28	0.63
	RF	0.74	0.54	1.63	0.71
	GB	0.65	0.38	1.85	0.68

Table S3. The evaluation metrics of molecules generated by VAE.

Metrics	**Validity↑**	**Uniqueness↑**	**Novelty↑**	**IntDiv↑**	**FCD↓**
Values	1	0.888	1	0.961	0.195

Table S4. The repeat unit of candidate polymer structures

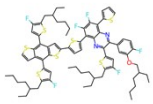	No.1 12.55	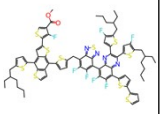	No.2 18.60	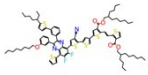	No.3 14.72	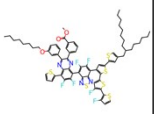	No.4 15.57
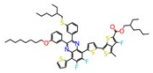	No.5 9.81	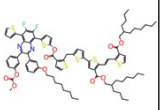	No.6 18.60	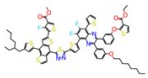	No.7 18.60	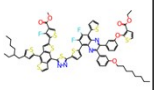	No.8 16.97
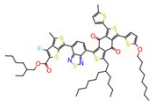	No.9 10.17	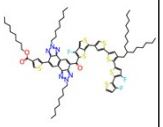	No.10 11.81	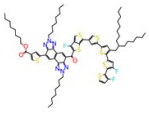	No.11 9.53	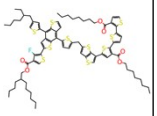	No.12 15.84
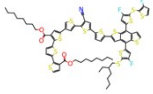	No.13 15.30	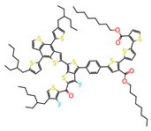	No.14 15.42	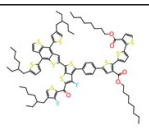	No.15 15.42	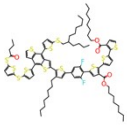	No.16 15.40
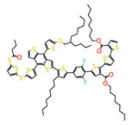	No.17 13.17	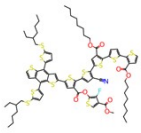	No.18 13.62	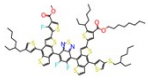	No.19 9.37	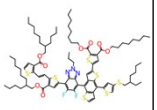	No.20 13.62
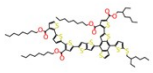	No.21 9.18	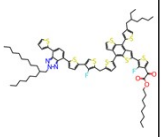	No.22 11.28	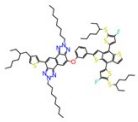	No.23 11.78	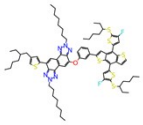	No.24 10.53
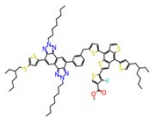	No.25 12.68	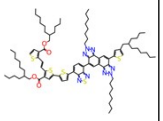	No.26 18.60	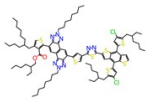	No.27 13.39	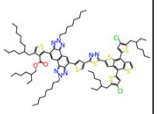	No.28 12.15
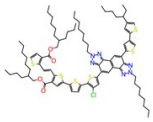	No.29 9.00	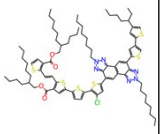	No.30 9.69	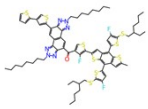	No.31 13.33	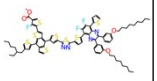	No.32 16.97
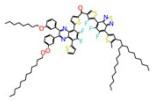	No.33 15.35	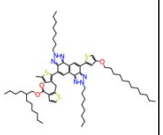	No.34 12.74	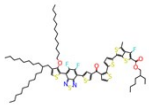	No.35 12.59	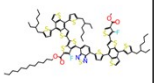	No.36 9.6
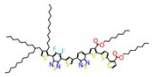	No.37 16.29		No.38 14.85	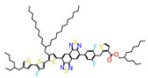	No.39 12.61	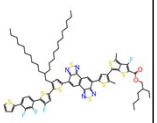	No.40 12.26

Continued Table S4.

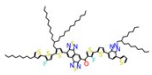	No.41 18.60	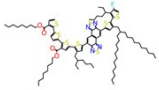	No.42 13.98	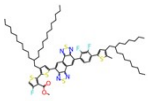	No.43 13.07	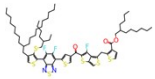	No.44 10.19
	No.45 11.27	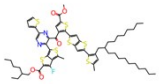	No.46 11.49	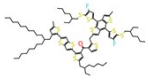	No.47 9.40	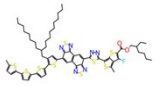	No.48 18.60
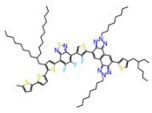	No.49 15.42	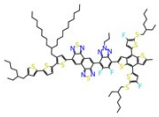	No.50 16.29	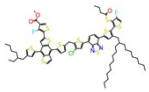	No.51 13.20	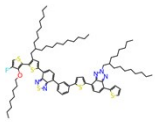	No.52 14.63
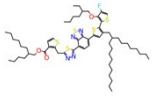	No.53 16.08	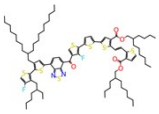	No.54 9.24	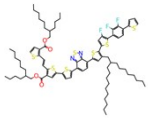	No.55 11.64	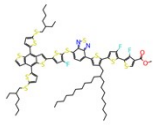	No.56 11.58
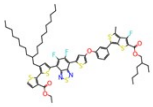	No.57 10.51	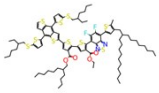	No.58 9.24	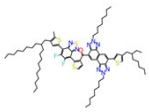	No.59 17.49	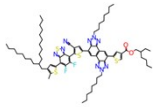	No.60 18.60
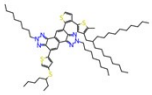	No.61 9.42	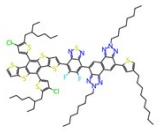	No.62 15.74	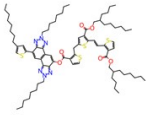	No.63 18.60	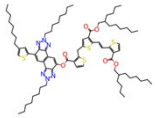	No.64 9.22
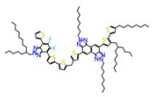	No.65 11.63	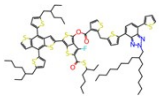	No.66 10.40	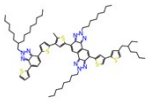	No.67 14.82	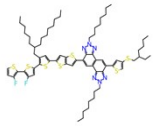	No.68 12.68
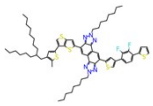	No.69 9.13	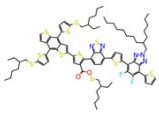	No.70 11.07	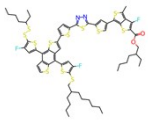	No.71 9.25	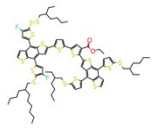	No.72 12.78
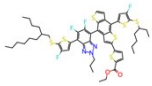	No.73 11.14	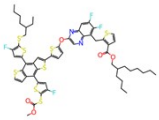	No.74 16.02	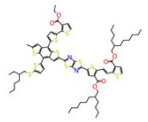	No.75 9.37	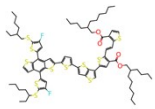	No.76 10.25
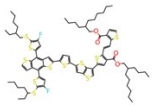	No.77 9.41	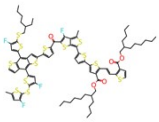	No.78 9.53	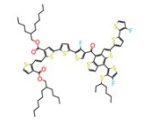	No.79 9.25	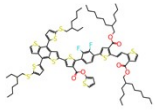	No.80 9.44

Continued Table S4.

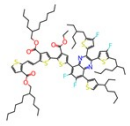	No.81 12.88	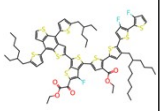	No.82 10.17	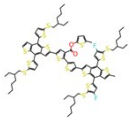	No.83 10.03	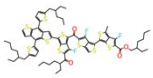	No.84 10.16
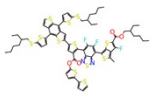	No.85 9.71	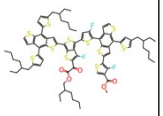	No.86 10.04		No.87 17.19		No.88 10.29
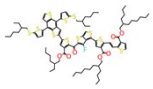	No.89 18.57	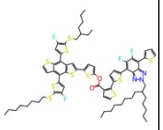	No.90 18.60				

Table S5. The detailed properties of selected candidates.

Descriptor	Candidate 1	Candidate 2
MolLogP	28.35	33.79
MolWt	1406.0	1658.4
NOCount	3	4
NumHAcceptors	10	10
NumHDonors	0	0
NumHeteroatoms	16	17
NumRotatableBonds	32	45
RingCount	11	11
NumAromaticHeterocycles	8	7
NumAromaticRings	11	11
SAscore	6.34	7.14
SCScore	4.99	4.99
DeepChemStable	0.968	0.968
DeepDonor	12.55	18.60

Table S6. Electrochemical properties of the candidates.

	E_{HOMO} (eV)	E_{LUMO} (eV)	E_g^{ec}(eV)
Candidate 1	-5.57	-3.58	1.99
Candidate 2	-5.59	-3.52	2.07
Candidate 1-1F	-5.58	-3.52	2.06
Candidate 1-0F	-5.49	-3.44	2.05

Table S7. New small molecule donor materials collected from literature to the end of 2021

Index	Voc	Jsc	FF	PCE	HOMO	LUMO	NAME	Reference
1	0.804	21.71	60.95	10.64	-5.021	-2.816	BTEC	1
2	0.87	21.21	61.35	11.33	-5.109	-2.853	BTEC-F	1
3	0.854	21.55	72.35	13.34	-5.116	-2.855	BTEC-2F	1
4	0.94	17.5	70.1	11.5	-5.36	-3.64	P2TBR	2
5	0.86	24.17	0.655	13.61	-5.46	-3.7	BTR-Cl	3
6	0.85	22.25	0.564	10.67	-5.34	-3.53	BTR	3
7	0.88	15.37	66.56	8.85	-5.05	-3.3	BDT-RO	4
8	0.81	22.2	0.608	10.9	-5.23	-3.59	FYSM-H	5
9	0.85	22.54	62.35	11.95	-5.37	-3.57	s35	6
10	0.97	14.86	0.63	9.03	-5.41	-2.9	BER6	7
11	0.96	11.1	0.51	5.52	-5.44	-2.99	BECN	7
12	0.87	22.5	0.69	13.35	-5.41	-3.57	BT-RO-Cl	8
13	0.87	22.93	0.7	13.9	-5.41	-3.58	BT-Reh-Cl	8
14	0.88	21.6	0.626	11.4	-5.29	-3.43	P-PHS	9
15	0.84	25.4	0.756	15.9	-5.34	-3.42	M-PHS	9
16	0.819	20.32	0.506	8.42	-5.39	-2.79	SM1-EH	10
17	0.766	22.39	0.684	11.73	-5.12	-2.8	SM1-Oct	10
18	0.829	17	0.413	5.82	-5.14	-3.44	3BDT-4	11
19	0.84	21.3	0.581	10.4	-5.15	-3.4	3BDT-5	11
20	1.057	15.07	0.568	9.05	-5.64	-3.61	DRTB-CT	12
21	0.85	22.3	0.69	13.1	-5.41	-3.5	TBD-S2	13
22	0.859	27.46	74.11	17.38	-5.5	-3.36	BTBR-2F	14
23	0.865	21.8	0.583	11	-5.59	3.69	B3T-T	15
24	0.813	25.6	0.717	14.9	-5.26	-3.65	B3T-P	15
25	0.88	23.2	0.68	13.9	-5.58	-3.59	BTTZR	16
26	0.849	21.77	0.6774	12.53	5.29	-3.13	FBD-S3	17
27	0.854	24.53	0.721	15.1	-5.31	-3.14	TBD-S4	17
28	0.969	17.24	0.64	10.76	-5.64	-3.61	DRTB-FT	18
29	0.885	19.78	0.688	12.02	-5.56	-3.6	ZR1-S-CL	19
30	0.774	24.5	0.726	13.76	-5.17	-3.43	BDTT-TR	20
31	0.805	23.59	0.67	12.72	-5.25	-2.78	SM1	21
32	0.825	23.23	0.677	12.94	-5.32	-2.81	SM1-S	21
33	0.866	23.25	0.699	14.07	-5.37	-2.81	SM1-F	21
34	0.865	20.1	0.713	12.4	-5.58	-3.39	BSCL-C2	22
35	0.865	21.5	0.7	13.03			BSCL	23
36	0.94	16.69	0.58	9.11	-5.44	-3.53	BDTF-CA	24
37	0.83	25.27	0.73	15.3	-5.37	-3.51	B1	25
38	0.861	24.34	68.44	14.34	-5.32	-3.53	ZR1	26
39	0.85	23.16	0.7	13.69	-5.59	-3.61	BSFTR	27
40	0.83	19.69	0.68	11.19	-6	-1.96	2CL7T	28

Continued Table S7

41	0.84	18.6	0.599	9.4	-5.27	-3.4	SE-1	29
42	0.87	19.42	0.612	10.3	-5.12	-3.44	SE-2	29
43	0.848	21.35	0.6512	11.79	-5.36	-3.55	ZR2-C1	30
44	0.852	23.03	0.6543	12.84	-5.35	-3.51	ZR2-C2	30
45	0.854	24.69	0.7	14.78	-5.34	-3.5	ZR2-C3	30
46	0.939	17.3	0.632	10.1	-5.43	-3.39	H13	31
47	0.943	18.3	0.7	12	-5.46	-3.47	H14	31
48	0.83	23.1	0.56	10.8	-5.4	-3.27	BOHTR	32
49	0.84	21.5	0.68	12.3	-5.36	-3.24	BIHTR	32
50	0.853	22.38	0.72	13.8	-5.4	-3.4	BT-2F	33
51	0.81	24.55	0.63	12.45	-5.05	-2.68	SM-DTBDT	34
52	0.84	21.63	0.588	10.68	-5.1	-2.7	SM-BDT	34
53	0.851	21.23	0.7256	13.1	-5.21	-3.55	SM8	35
54	0.837	19.2	0.659	10.5	-5.23	-3.57	SM12	35
55	0.88	23.2	0.68	13.9	-5.58	-3.59	SL1	36
56	0.89	21.6	0.6	11.5	-5.6	-3.62	SL2	36
57	0.88	21.6	0.67	12.7	-5.58	-3.6	SL3	36
58	0.87	23	0.62	12.4	-5.57	-3.57	SL4	36
59	0.784	24.59	0.7278	14.03	-5.17	-3.43	TBFT-TR	20
60	0.95	15.72	0.626	10.4	-5.4	-3.24	DRTT-R	37

Table S8. New polymer molecule donor materials collected from literature to the end of 2021

ID	PCE	Voc	Jsc	FF	HOMO	LUMO	NAME	Reference
1	15.55	0.844	26.02	0.71	-5.55	-2.91	PBQ5	38
2	17.62	0.851	26.58	0.78	-5.64	-3.18	PBQ6	38
3	7.16	0.82	13.76	0.64	-5.24	-3.55	PDTBDT-SBTEH	39
4	8.61	0.94	13.81	0.66	-5.43	-3.67	PDTBDT-SFBTEH	39
5	11.47	0.9	21.86	0.59	-5.6	-3.49	PBDTT2Cl	40
6	17.1	0.87	27.7	0.71	-5.47	-3.48	PBDTT1Cl	40
7	10.9	0.92	17.5	0.68	-5.52	-3.65	PBSF-A12	41
8	13.4	0.92	20.5	0.71	-5.5	-3.59	PBSF-D12	41
9	16.1	0.88	25.2	0.72			PBNT-BDD	42
10	8.22	0.895	17.18	0.54	-5.67	-3.28	PDTBDT	43
11	12.71	0.78	24.21	0.66	-5.4	-3.21	PDTBDT-T	43
12	15.63	0.86	24.46	0.72	-5.58	-3.26	PDTBDT-T-Cl	43
13	11.5	0.87	18.83	0.70	-5.5	-3.74	PV2TC-BDD	44
14	8.56	0.71	20.49	0.59	-5.35	-3.56	PV2TC-FTAZ	44
15	5.89	0.86	13.87	0.49	-4.34	-2.16	PvBDT-F	45
16	7.76	0.9	15.04	0.57	-4.4	-2.24	PvBDT-Cl	45
17	17.1	0.85	27.2	0.74	-5.58	-3.66	PBCT-2F	46
18	17.21	0.85	25.81	0.79	-5.44	-3.47	D18	47
19	17.97	0.87	26.83	0.77	-5.46	-3.49	D18-Cl	47
20	10.08	1.11	13.68	0.66	-5.35	-3.54	PE31	48
21	7.4	1.1	11.65	0.58	-5.22	-3.3	PE32	48
22	8.99	1.16	12.68	0.61	-5.42	-3.55	PE33	48
23	8.64	1.21	11.36	0.63	-5.46	-3.58	J52-CL	48
24	9.7	0.9	16.1	0.67	-5.66	-3.88	PM6F	49
25	15.3	0.92	21.2	0.79	-5.6	-3.52	PFBCPZ	50
26	12.81	0.89	19.91	0.72	-5.33	-3.43	PFBDT-8ttTPD	51
27	15.05	0.84	24.99	0.72	-5.46	-3.57	PClBDT-8ttTPD	51
28	13.1	0.88	20.5	0.72	-5.4	-3.6	PBDB-T-SF	52
29	11.62	0.73	21.63	0.74	-5.35	-3.43	P4T2F-HD	53
30	16.32	0.88	24.79	0.75	-5.52	-2.76	PTQ11	54
31	13.45	0.81	25.83	0.64	-5.38	-3.14	PBQ7	55
32	16.34	0.85	25.77	0.75	-5.47	-2.89	PBQ510	55
33	15.1	0.83	23.9	0.76	-5.48	-3.68	PBTT-F	56
34	7.58	0.865	12.4	0.71	-5.37	-3.63	PBNS	57
35	14.86	0.83	25.36	0.68	-5.51	-3.64	PBDT-F	58
36	15.63	0.85	25.69	0.71	-5.53	-3.64	PBDT-Cl	58
37	11.58	0.74	24.91	0.63	-5.35	-3.48	PBDT-H	58
38	14.35	0.915	22.56	0.70	-5.43	-3.54	PBDT-ST	59
39	13.72	0.896	22.67	0.68	-5.47	-3.57	PNDT-ST	59
40	11.39	1.01	17.89	0.63	-5.6	-3.65	P1	60

Table S9. The structures and appearance times of cores and side-chains

Dataset	Structure	Substructures and the appearance times
PM	cores	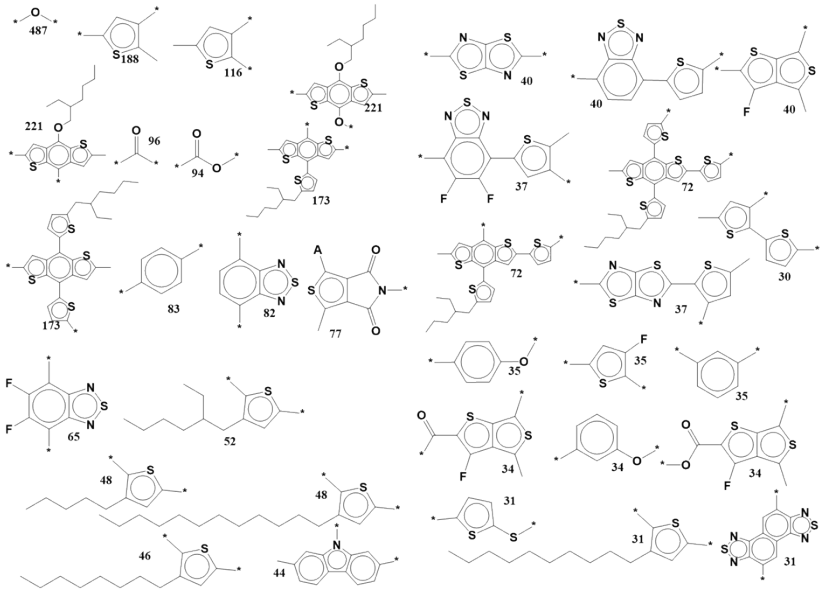
PM	side-chains	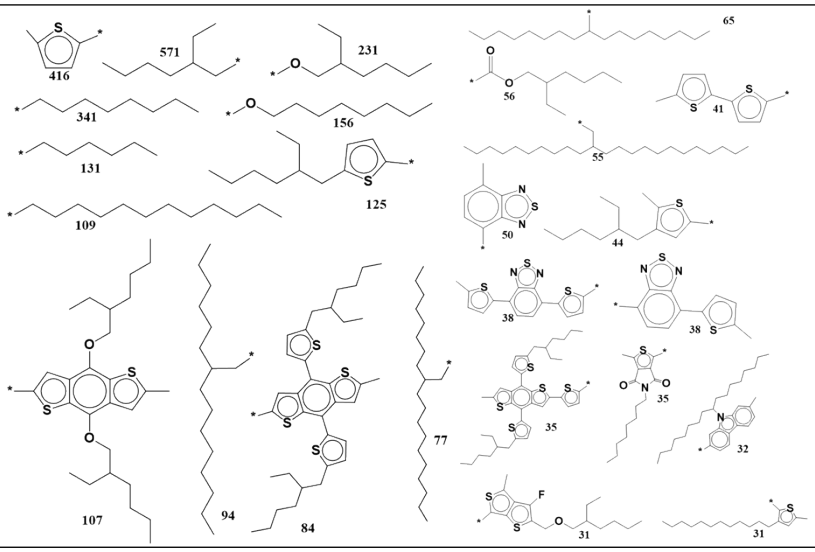

Continued Table S9

SM	cores	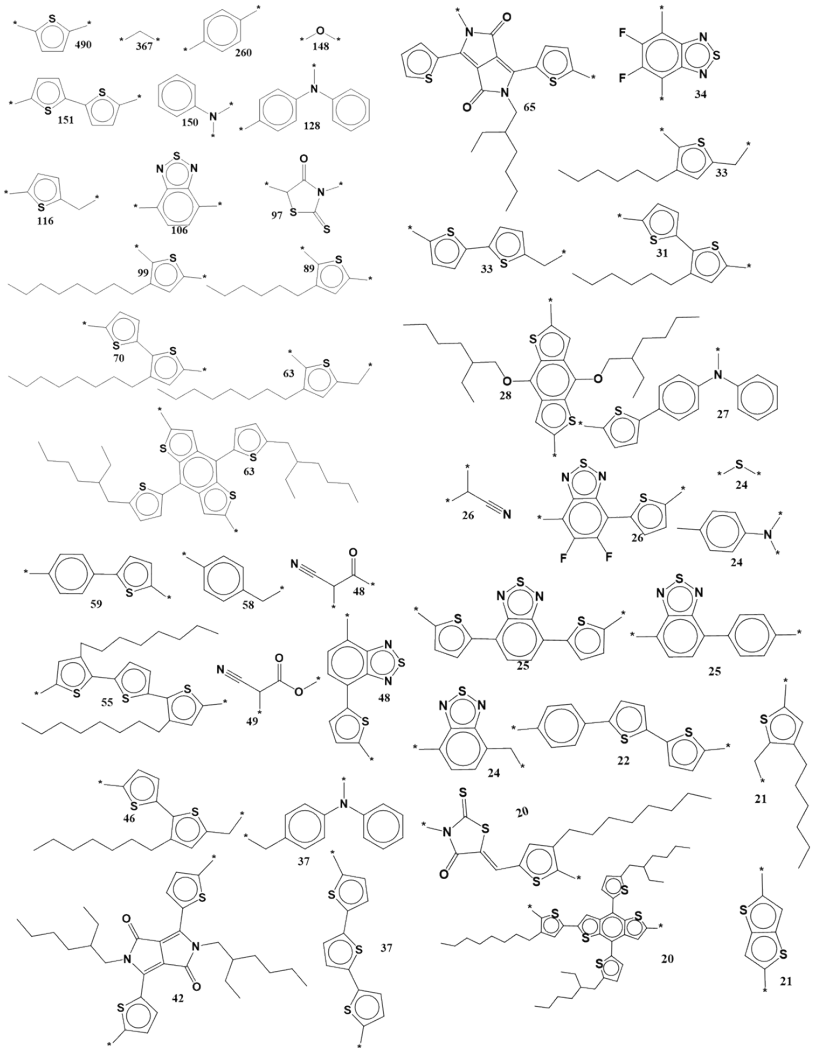
SM	side-chains	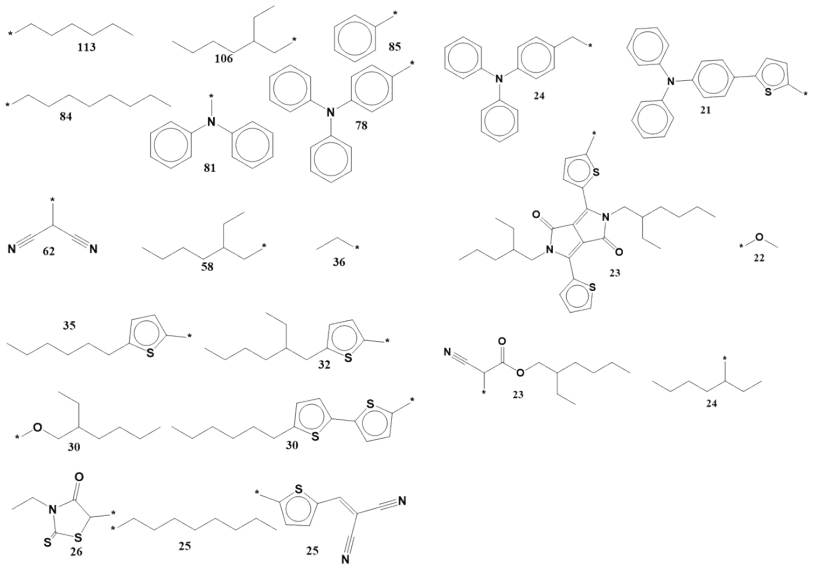

Table S10. New small molecule donor materials collected from literature from 2022 and 2023.

Name	HOMO	LUMO	Voc	Jsc	FF	PCE	Reference
W2-CA	-5.17	-3.53	0.83	25.19	76.8	16.06	61
W2-Reh	-5.16	-3.48	0.826	25.31	74.8	15.63	61
BBTSM-1	−5.58	−3.51	0.87	21.6	63	11.8	62
Tz6T-iP	−5.29	−3.64	849.1	25.55	72.49	15.7	63
Tz6T-P	−5.37	−3.76	876.1	24.83	67.4	14.7	63
MPhS-C2			0.867	24.42	74.08	15.67	64
MPhS-Ph			0.859	23.63	72.75	14.77	64
CBTSeEHR	−5.45	−3.61	0.881	18.76	0.732	12.1	65
BTEHR-CTb	−5.56	−3.47	0.908	17.43	0.685	10.84	65
CBTSeHR	−5.47	−3.62	0.871	15.28	0.698	9.3	65
C3-CN	−5.38	-3.42	1.05	20.54	0.68	14.62	66
C3	-5.28	−3.09	0.96	18.41	0.62	10.85	66
SM-REH			0.85	25.42	72.4	15.6	67
SM-EH-R			0.85	23.73	71.3	14.4	67
SM-R			0.86	24.64	66.2	14	67
SM-EH-R			0.85	21.96	63.4	11.9	67
DRTT-6Se	−5.54	−3.44	0.85	25.29	69.9	15.03	68
DRTT-2Se	−5.51	−3.46	0.85	25.18	68.8	14.79	68
DRTT-T	−5.57	−3.36	0.85	24.85	62.9	13.37	68
As-TCp	−5.30	−2.78	0.873	24.45	74.9	16.46	69
S-TCp	−5.27	−2.76	0.87	23.88	73.83	15.77	69
S-BF	−5.32	−2.80	0.868	22.91	69.39	14.92	69
SM-*s*-Bu	−5.24	−3.53	0.841	25.18	74.34	16.06	70
SM-*n*-Bu	−5.19	−3.61	0.83	24.75	72.12	15.12	70
BTEHR-CT	-5.56	-3.47	0.946	17.05	0.69	11.13	71
a-BTR-H4	−5.30	−3.54	0.815	24.8	53.5	11.36	72
SW2	− 5.47	− 3.45	0.835	74	25.1	15.51	73
SW1	− 5.42	− 3.43	0.806	63.8	25.09	12.9	73
TBCA-C4	−5.49	−3.46	0.933	15.43	0.64	9.21	74

Table S11. New polymer molecule donor materials collected from literature from 2022 and 2023.

Name	HOMO	LUMO	Voc	Jsc	FF	PCE	Reference
PBT	−5.45	−3.37	0.79	25.6	63.3	12.90	75
PiBT	−5.53	−3.17	0.87	28.2	77.3	19.00	75
PTO-HD	−5.51	−3.58	0.806	23.24	74.19	13.89	76
PTO-BO	−5.47	−3.61	0.799	22.74	67.67	12.29	76
PQx4T-2F	−5.40	−3.45	0.84	25.78	73.65	15.95	77
PQx4T	−5.30	−3.35	0.82	24.82	65.37	13.30	77
PBDTF-ttPTZ			0.715	23.87	65.60	11.03	78
PJ-1	−5.54	-3.54	0.864	66.1	26.08	15.01	79
PBTID	-5.53	-3.54	0.87	26.1	69.6	15.80	80
PDTBTBz-2F	-5.56	–3.64	0.87	21.69	65.5	12.37	81
PDTBTBz-2H	-5.42	–3.45	0.77	21.82	57.6	9.73	81
PBDT-PiQ	−5.40	−3.34	0.85	20.82	63.51	11.28	82
PNDT2			0.861	26.33	80	18.13	83
PNDT1			0.865	25.85	77.2	17.27	83
PBN-SBO	−5.39	−3.58	0.851	25.84	73.8	16.22	84
PBN-S	−5.33	−3.48	0.848	24.71	61.4	12.86	84
PZ2	-5.48	-3.69	0.817	60.01	22.88	11.21	85
PZ3	-5.5	-3.68	0.83	60.5	21.44	10.77	85
Z4	–5.59	–3.41	0.807	26.27	71.06	15.12	86
Z3	–5.42	–3.38	0.798	20.07	66.71	10.68	86
PBDQx-β-Cl	–5.64	–3.93	0.85	24.84	68.33	14.49	87
PTzBTE	-5.47	-3	0.87	23.8	72	14.90	88
P3	−5.38	−3.51	0.742	22.8	74.3	12.56	89
P1	−5.41	−3.49	0.766	18.12	73.72	10.37	89
P(TPTI-BDT)	−5.30	−3.26	0.86	20	70	11.70	90
P(2DTP-BDT)	−5.35	−3.38	0.93	15.8	68	9.20	90
PSe-HD	–5.50	–3.49	0.852	25.76	67.66	14.85	91
PSe-BO	–5.45	–3.29	0.845	23.63	65.48	13.07	91
PM6-F	-5.62	-3.74	0.93	21.71	66.56	13.44	92
PFNT-Cl	-5.51	-3.53	0.842	26.03	80	17.53	93
PTTB-F			0.882	26.56	77.08	18.06	94
PTTB-H			0.827	24.49	65.88	13.34	94
PBDF-TF-BTz			0.857	24.8	77.78	17.01	95
BDF-dT-BTz			0.852	24.32	75.21	16.03	95
PBDF-dF-BTz			0.863	23.08	74.42	15.59	95
J52-FTh	−5.51	−3.68	0.92	21.29	68	13.32	96
PNTB-HD			0.854	26.88	79	18.15	97
PNTB-2T			0.841	26.07	76.5	16.77	97
PBTTz3Cl	-5.56	-3.6	0.888	26.6	77.81	18.38	98

Continued Table S11

PBTz-TC	−5.47	−3.52	0.84	20.91	72.69	12.81	99
PBTz-TTC	−5.38	−3.51	0.84	18.47	61.4	9.52	99
PM7-F	−5.65	−3.75	0.94	20.79	68.87	13.46	100
P126	−5.53	−3.35	0.89	23.52	72	15.07	101
P127	−5.47	−3.34	0.82	22.24	67	12.27	101
PBDT-2FBn	−5.52	−3.50	0.858	18	60.2	9.30	102
L3			0.864	26.97	76.4	17.81	103
PNBTz1	-5.44	-5.288	0.85	24	72	14.00	104
PL2	−5.49	−3.98	0.69	23.3	62.66	10.12	105

Supplementary Note 1

1. Device Fabrication

The OSC devices were fabricated with a structure of ITO/PEDOT:PSS/Photoactive layer/PFN-Br/Ag. The ITO substrates (10 Ω sq^{-1}) were cleaned by sequential ultrasonic treatment in detergent, deionized water, and isopropanol. Then, the dried ITO substrates were treated with an ultraviolet-ozone chamber for 25 min. A thin layer of PEDOT: PSS was prepared on precleaned ITO glass through spin-coating a PEDOT: PSS aqueous solution (Heraeus-Clevios PVP Al 4083 from Xi'an Polymer Light Technology Corp. (China)) at 5000 rpm and baked subsequently at 140°C for 15 min in the air. The substrates were then transferred into an N_2-filled glovebox. A blend solution was prepared by dissolving the polymer donor and acceptor in chloroform with the same optimal donor/acceptor (D/A) weight ratios of 1:1.2 for blends with a total concentration of 16 mg/mL with 0.35% DIO by volume, and then the blend solution was spin-coated at 2500 rpm onto the PEDOT: PSS layer. After spin-coating, the active layers were annealed at 95°C for 10 min. Then, the methanol solution of PFN-Br at a concentration of 0.5 mg mL^{-1} is spin-coated at 3000 rpm to afford a cathode buffer layer. Finally, cathode metal Ag was deposited. The photoactive layer effective area of the device was 4.8 mm^2.

2. Synthesis of monomers and polymers

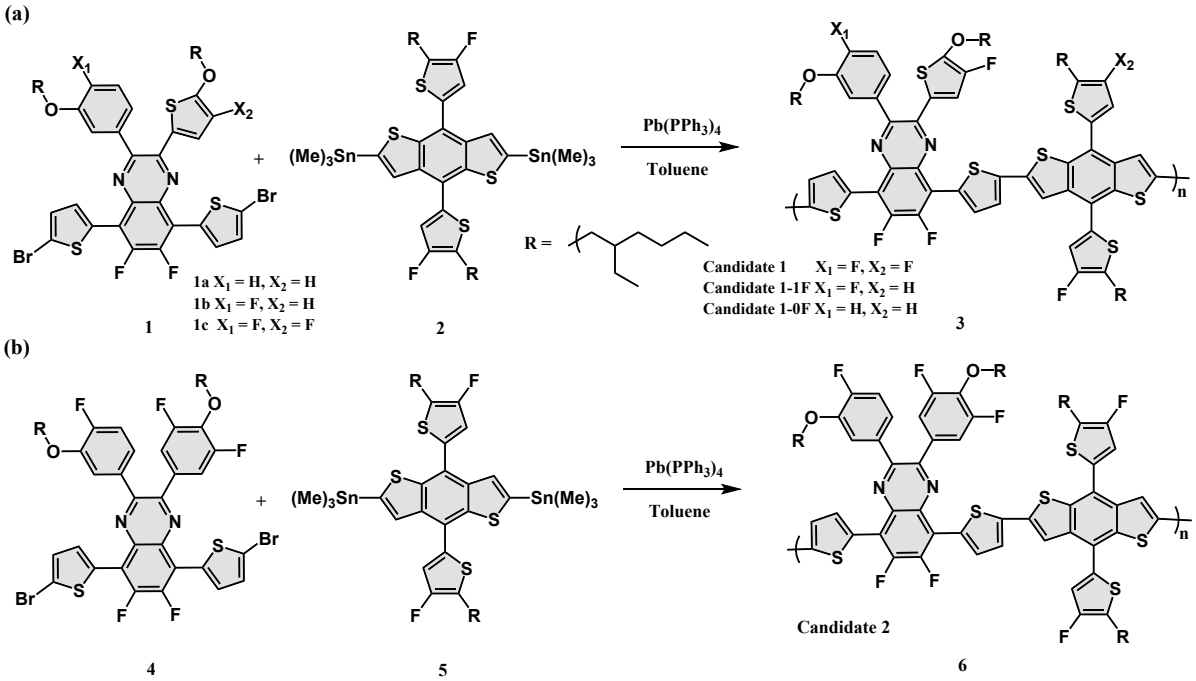

Figure S6. Synthetic route of the (a) Candidate 1 and (b) candidate 2.

Candidate 1, 1-0F and 1-1F have been published in our recent work.[106]

Candidate 1-0F: 1a (129 mg, 0.145 mmol), :4,8-Bis-[5-(2-ethyl-hexyl)-4-fluoro-thiophen-2-yl]-2,6-bis-trimethylstannanyl-1,5-dithia-s-indacene (136.8 mg, 0.145 mmol), and Pd(PPh3)4 (4.2 mg, 0.004 mmol) were dissolved in 10 mL toluene and refluxed for 36h. After cooling down to room temperature, the mixture was poured into the 100 mL methanol and then stirred for 0.5h. Whereafter the precipitate was collected and extracted in the order of methanol, hexane, acetone, and chloroform. Subsequently, the polymer solution was removed chloroform solvent by rotary evaporation to obtain atropurpureus lamellar solid Candidate **1-0F** (129 mg, 67 %)).

Candidate 1-1F and **Candidate 1** were obtained with compound **1b** (0.162 g, 0.179 mmol) and **1c** (0.156 g, 0.169 mmol) following the general procedure described above. (Atropurpureus lamellar solid, 172 mg, 71 % and 183 mg, 78 %), respectively.

Candidate 2 :4 (137.8 mg, 0.145 mmol), :**5** (4,8-Bis-[5-(2-ethyl-hexyl)-4-fluoro-thiophen-2-yl]-2,6-bis-trimethylstannanyl-1,5-dithia-s-indacene) (136.8 mg, 0.145 mmol), and $Pd(PPh_3)_4$ (4.2 mg, 0.004 mmol) were dissolved in 10 mL toluene and refluxed for 24 h. After cooling down to room temperature, the mixture was poured into the 100 mL methanol and then stirred for 0.5h. Whereafter the precipitate was collected and extracted in the order of methanol, hexane, acetone, and chloroform. Subsequently, the polymer solution was removed chloroform solvent by rotary evaporation to obtain atropurpureus lamellar solid **Candidate 2** (140 mg, 68 %).

References

1. Ge, J. et al. 13.34 % Efficiency Non-Fullerene All-Small-Molecule Organic Solar Cells Enabled by Modulating the Crystallinity of Donors via a Fluorination Strategy. Angewandte Chemie International Edition 59, 2808–2815 (2020).
2. Li, X. et al. A small molecule donor containing a non-fused ring core for all-small-molecule organic solar cells with high efficiency over 11%. J. Mater. Chem. A 7, 3682–3690 (2019).
3. Chen, H. et al. All-Small-Molecule Organic Solar Cells with an Ordered Liquid Crystalline Donor. Joule 3, 3034–3047 (2019).
4. Duan, T. et al. Terminal group engineering for small-molecule donors boosts the performance of nonfullerene organic solar cells. J. Mater. Chem. A 7, 2541–2546 (2019).
5. Su, W. et al. 13.4 % Efficiency from All-Small-Molecule Organic Solar Cells Based on a Crystalline Donor with Chlorine and Trialkylsilyl Substitutions. ChemSusChem 14, 3535–3543 (2021).
6. Wang, Q. et al. Introducing Siloxane-Terminated Side Chains in Small Molecular Donors for All-Small-Molecule Organic Solar Cells: Modulated Molecular Orientation and Enhanced Efficiency. ACS Appl. Mater. Interfaces 13, 36080–36088 (2021).
7. Zhao, J. et al. Wide-Band Gap Small-Molecule Donors with Diester-Terthiophene Bridged Units for High-Efficiency All-Small-Molecule Organic Solar Cells. ACS Appl. Energy Mater. 4, 5868–5876 (2021).
8. Chen, H. et al. Design of All-Small-Molecule Organic Solar Cells Approaching 14% Efficiency via Isometric Terminal Alkyl Chain Engineering. Energies 14, 2505 (2021).
9. Zhang, L. et al. High Miscibility Compatible with Ordered Molecular Packing Enables an Excellent Efficiency of 16.2% in All-small-molecule Organic Solar Cells. Advanced Materials n/a, 2106316.
10. Shi, K. et al. Effects of Alkyl Side Chains of Small Molecule Donors on Morphology and the Photovoltaic Property of All-Small-Molecule Solar Cells. ACS Appl. Mater. Interfaces 13, 54237–54245 (2021).
11. Yang, D. et al. Achieving 10% efficiency in non-fullerene all-small-molecule organic solar cells without extra treatments. J. Mater. Chem. A 9, 10427–10436 (2021).

12. Qiu, N. et al. Improving the performances of all-small-molecule organic solar cells by fine-tuning halogen substituents of donor molecule. Organic Electronics 99, 106340 (2021).
13. Wang, X. et al. Backbone Engineering with Asymmetric Core to Finely Tune Phase Separation for High-Performance All-Small-Molecule Organic Solar Cells. ACS Appl. Mater. Interfaces 13, 11108–11116 (2021).
14. Xu, L. et al. Achieving 17.38% efficiency of ternary organic solar cells enabled by a large-bandgap donor with noncovalent conformational locking. J. Mater. Chem. A 9, 11734–11740 (2021).
15. An, C. et al. Optimization of active layer morphology by small-molecule donor design enables over 15% efficiency in small-molecule organic solar cells. J. Mater. Chem. A 9, 13653–13660 (2021).
16. Wang, Y. et al. A novel wide-bandgap small molecule donor for high efficiency all-small-molecule organic solar cells with small non-radiative energy losses. Energy Environ. Sci. 13, 1309–1317 (2020).
17. Wang, X. et al. Over 15% efficiency all-small-molecule organic solar cells enabled by a C-shaped small molecule donor with tailorable asymmetric backbone. Nano Energy 81, 105612 (2021).
18. Liu, C. et al. All-Small-Molecule Organic Solar Cells Based on a Fluorinated Small Molecule Donor With High Open-Circuit Voltage of 1.07 V. Frontiers in Chemistry 8, 329 (2020).
19. Zhou, R. et al. Combining chlorination and sulfuration strategies for high-performance all-small-molecule organic solar cells. Journal of Energy Chemistry 52, 228–233 (2021).
20. Sun, R. et al. High-efficiency all-small-molecule organic solar cells based on an organic molecule donor with an asymmetric thieno[2,3-f] benzofuran unit. Sci. China Chem. 63, 1246–1255 (2020).
21. Qiu, B. et al. Highly Efficient All-Small-Molecule Organic Solar Cells with Appropriate Active Layer Morphology by Side Chain Engineering of Donor Molecules and Thermal Annealing. Advanced Materials 32, 1908373 (2020).
22. Wu, Q. et al. Modulation of Donor Alkyl Terminal Chains with the Shifting Branching Point Leads to the Optimized Morphology and Efficient All-Small-Molecule Organic Solar Cells. ACS Appl. Mater. Interfaces 12, 25100–25107 (2020).
23. Zhang, Z. et al. The post-treatment effects on open circuit voltages and device performances in a high efficiency all-small-molecule organic solar cell. J. Mater. Chem. C 8, 15385–15392 (2020).
24. Wu, Q. et al. Fluorination-substitution effect on all-small-molecule organic solar cells. Sci. China Chem. 62, 837–844 (2019).
25. Qin, J. et al. 15.3% efficiency all-small-molecule organic solar cells enabled by symmetric phenyl substitution. Sci. China Mater. 63, 1142–1150 (2020).
26. Zhou, R. et al. All-small-molecule organic solar cells with over 14% efficiency by optimizing hierarchical morphologies. Nat Commun 10, 5393 (2019).
27. Yue, Q. et al. 13.7% Efficiency Small-Molecule Solar Cells Enabled by a Combination of Material and Morphology Optimization. Advanced Materials 31, 1904283 (2019).
28. Duan, T. et al. Simple organic donors based on halogenated oligothiophenes for all small molecule solar cells with efficiency over 11%. J. Mater. Chem. A 8, 5843–5847 (2020).
29. Li, Y. et al. Efficient charge generation and low open circuit voltage loss enable a PCE of 10.3% in small molecule donor and polymer acceptor organic solar cells. J. Mater. Chem. C (2021) doi:10.1039/D1TC04428A.
30. Zhou, R. et al. Moving Alkyl-Chain Branching Point Induced a Hierarchical Morphology for Efficient All-Small-Molecule Organic Solar Cells. Advanced Functional Materials 30, 2005426 (2020).
31. Bin, H. et al. Precise Control of Phase Separation Enables 12% Efficiency in All Small Molecule Solar Cells. Advanced Energy Materials 10, 2001589 (2020).

32. Dong, X. et al. Improving Molecular Planarity by Changing Alky Chain Position Enables 12.3% Efficiency All-Small-Molecule Organic Solar Cells with Enhanced Carrier Lifetime and Reduced Recombination. Sol. RRL 4, 1900326 (2020).
33. Gao, J. et al. Over 14% efficiency nonfullerene all-small-molecule organic solar cells enabled by improving the ordering of molecular donors via side-chain engineering. J. Mater. Chem. A 8, 7405–7411 (2020).
34. Li, S. et al. Effects of the Center Units of Small-Molecule Donors on the Morphology, Photovoltaic Performance, and Device Stability of All-Small-Molecule Organic Solar Cells. Sol. RRL 5, 2100515 (2021).
35. Guo, J. et al. Fine-Tuning Miscibility and π–π Stacking by Alkylthio Side Chains of Donor Molecules Enables High-Performance All-Small-Molecule Organic Solar Cells. ACS Appl. Mater. Interfaces 13, 36033–36043 (2021).
36. Wang, Y. et al. Modulating Crystallinity and Miscibility via Side-chain Variation Enable High Performance All-Small-Molecule Organic Solar Cells. Chinese Journal of Chemistry 39, 2147–2153 (2021).
37. Cheng, X. et al. "Twisted" conjugated molecules as donor materials for efficient all-small-molecule organic solar cells processed with tetrahydrofuran. J. Mater. Chem. A 7, 23008–23018 (2019).
38. Zhu, C. et al. A Quinoxaline-Based D–A Copolymer Donor Achieving 17.62% Efficiency of Organic Solar Cells. Advanced Materials 33, 2100474 (2021).
39. Gong, P. et al. Ultrafast Kinetics Investigation of a Fluorinated-Benzothiadiazole Polymer with an Increased Excited State Transition Dipole Moment Applied in Organic Solar Cells. ACS Appl. Energy Mater. 4, 9627–9638 (2021).
40. Wang, H. et al. Chlorination Enabling a Low-Cost Benzodithiophene-Based Wide-Bandgap Donor Polymer with an Efficiency of over 17%. Advanced Materials n/a, 2105483.
41. Wang, K. et al. Optimizing the Alkyl Side-Chain Design of a Wide Band-Gap Polymer Donor for Attaining Nonfullerene Organic Solar Cells with High Efficiency Using a Nonhalogenated Solvent. Chem. Mater. 33, 5981–5990 (2021).
42. Pang, S. et al. A Facile Synthesized Polymer Featuring B-N Covalent Bond and Small Singlet-Triplet Gap for High-Performance Organic Solar Cells. Angewandte Chemie International Edition 60, 8813–8817 (2021).
43. Tang, Y. et al. Optimizing the energy levels and crystallinity of 2,2′-bithiophene-3,3′-dicarboximide-based polymer donors for high-performance non-fullerene organic solar cells. J. Mater. Chem. C 9, 7575−7582 (2021).
44. Liu, Z. et al. Novel efficient accptor1-acceptor2 type copolymer donors: Vinyl induced planar geometry and high performance organic solar cells. Chemical Engineering Journal 419, 129532 (2021).
45. Zhang, M., Xu, X., Yu, L. & Peng, Q. Efficient wide-band-gap copolymer donors for organic solar cells with perpendicularly placed benzodithiophene units. Journal of Power Sources 499, 229961 (2021).
46. Yuan, X. et al. A donor polymer based on 3-cyanothiophene with superior batch-to-batch reproducibility for high-efficiency organic solar cells. Energy Environ. Sci. 14, 5530–5540 (2021).
47. Zeng, A. et al. A Chlorinated Donor Polymer Achieving High-Performance Organic Solar Cells with a Wide Range of Polymer Molecular Weight. Advanced Functional Materials 31, 2102413 (2021).
48. Dai, T. et al. Fabrication of High VOC Organic Solar Cells with a Non-Halogenated Solvent and the Effect of Substituted Groups for "Same-A-Strategy" Material Combinations. ACS Appl. Mater. Interfaces 13, 21556–21564 (2021).
49. Guo, Q. et al. Optimized molecular aggregation via incorporating fluorinated unit in the polymer donor for 17.3% efficiency organic solar cells. Chemical Engineering Journal 134117 (2021) doi:10.1016/j.cej.2021.134117.
50. Wu, J. et al. Carboxylate substituted pyrazine: A simple and low-cost building block for novel wide bandgap polymer donor enables 15.3% efficiency in organic solar cells. Nano Energy 82, 105679 (2021).

51. Ha, J.-W. et al. Highly Efficient and Photostable Ternary Organic Solar Cells Enabled by the Combination of Non-Fullerene and Fullerene Acceptors with Thienopyrrolodione-based Polymer Donors. ACS Appl. Mater. Interfaces 12, 51699–51708 (2020).
52. Zhao, W. et al. Molecular Optimization Enables over 13% Efficiency in Organic Solar Cells. J. Am. Chem. Soc. 139, 7148–7151 (2017).
53. Xiao, J. et al. Surpassing 13% Efficiency for Polythiophene Organic Solar Cells Processed from Nonhalogenated Solvent. Advanced Materials 33, 2008158 (2021).
54. Sun, C. et al. High Efficiency Polymer Solar Cells with Efficient Hole Transfer at Zero Highest Occupied Molecular Orbital Offset between Methylated Polymer Donor and Brominated Acceptor. J. Am. Chem. Soc. 142, 1465–1474 (2020).
55. Sun, C. et al. D–A Copolymer Donor Based on Bithienyl Benzodithiophene D-Unit and Monoalkoxy Bifluoroquinoxaline A-Unit for High-Performance Polymer Solar Cells. Chem. Mater. 32, 3254–3261 (2020).
56. Chao, P. et al. A Benzo[1,2-b:4,5-c′]Dithiophene-4,8-Dione-Based Polymer Donor Achieving an Efficiency Over 16%. Advanced Materials 32, 1907059 (2020).
57. Wang, Q. et al. Naphtho[2,3-c]thiophene-4,9-dione based polymers for efficient fullerene solar cells. Polymer 212, 123184 (2021).
58. Park, J. S. et al. Importance of Optimal Crystallinity and Hole Mobility of BDT-Based Polymer Donor for Simultaneous Enhancements of Voc, Jsc, and FF in Efficient Nonfullerene Organic Solar Cells. Advanced Functional Materials 30, 2005787 (2020).
59. Xu, X. et al. Subtle Polymer Donor and Molecular Acceptor Design Enable Efficient Polymer Solar Cells with a Very Small Energy Loss. Advanced Functional Materials 30, 1907570 (2020).
60. Tang, Y. et al. A New Wide Bandgap Donor Polymer for Efficient Nonfullerene Organic Solar Cells with a Large Open-Circuit Voltage. Advanced Science 6, 1901773 (2019).
61. Wang, Q. et al. Synergy Effect of Symmetry-Breaking and End-Group Engineering Enables 16.06% Efficiency for All-Small-Molecule Organic Solar Cells. ACS Materials Lett. 6, 713–719 (2024).
62. Han, D. et al. Small molecular donor materials based on electron withdrawing benzobisthiazole core unit enable an efficiency of 11.8% for organic solar cells. Chemical Engineering Journal 463, 142400 (2023).
63. Chen, Q., Li, Y., Hu, D., Lu, S. & Xiao, Z. Branched Terminal Alkyl Chain Enabling 15.7% Efficiency Oligothiophene Donor. Solar RRL 8, 2300802 (2024).
64. Ma, X. et al. Small Molecule Donors Design Rules for Non-Halogen Solvent Fabricated Organic Solar Cells. Small n/a, 2309042.
65. Liu, C., Wu, Z., Qiu, N., Li, C. & Lu, Y. Selenophene-containing benzodithiophene based donors with different alkyl chains in terminal groups for high-performance all-small-molecule organic solar cells. New J. Chem. 47, 2840–2846 (2023).
66. Pradhan, R. et al. Achieving High-Efficiency in Binary Organic Solar Cells by the Structural Fine-Tuning of Coumarin-Based Donor. Solar RRL 7, 2300032 (2023).
67. Ge, J. et al. Modulation of Molecular Stacking via Tuning 2-Ethylhexyl Alkyl Chain Enables Improved Efficiency for All-Small-Molecule Organic Solar Cells. ACS Appl. Mater. Interfaces 15, 10803–10811 (2023).
68. Cheng, X. et al. “Twisted” small molecule donors with enhanced intermolecular interactions in the condensed phase towards efficient and thick-film all-small-molecule organic solar cells. J. Mater. Chem. A 11, 13984–13993 (2023).
69. Wang, X. et al. High-Efficiency All-Small-Molecule Organic Solar Cells Based on New Molecule Donors with Conjugated Symmetric/Asymmetric Hybrid Cyclopentyl-Hexyl Side Chains. Advanced Functional Materials 33, 2300323 (2023).

70. Zhi, H.-F. et al. Isomeric Small Molecule Donor with Terminal Branching Position Directly Attached to the Backbone Enables Efficient All-Small-Molecule Organic Solar Cells with Excellent Stability. Advanced Functional Materials 33, 2300878 (2023).
71. Liu, C. et al. A novel chlorinated small molecule donor for efficient binary and ternary all-small-molecule organic solar cells. Organic Electronics 106, 106532 (2022).
72. Zhao, Y. et al. End Group Effect of Asymmetric Benzodithiophene-Based Donor with Liquid-Crystal State for Small-Molecule Binary Solar Cell. Small 19, 2205244 (2023).
73. Wu, S. et al. 15.51 % efficiency all-small-molecule organic solar cells achieved by symmetric thiazolyl substitution. Nano Energy 103, 107801 (2022).
74. Yang, L. et al. Terminal alkyl chain tuning of small molecule donor enables optimized morphology and efficient all-small-molecule organic solar cells. Dyes and Pigments 200, 110147 (2022).
75. Lin, T. et al. Isomerization of Benzothiadiazole Yields a Promising Polymer Donor and Organic Solar Cells with Efficiency of 19.0%. Advanced Materials n/a, 2312311.
76. Hu, L., Wang, L., Ye, L., Zhao, B. & Tan, S. Polymer donors based on alkyloxime-substituted thiophene and 6-undecylthiopheno[3,2-b]thiophene for efficient organic solar cells. Journal of Polymer Science (2024) doi:10.1002/pol.20230883.
77. Wang, X. et al. Dithienoquinoxaline-quaterthiophene wide bandgap donor polymers with strong interchain aggregation for efficient organic solar cells processed with a non-halogenated solvent. J. Mater. Chem. A (2024) doi:10.1039/D3TA08020J.
78. Xu, G. et al. Novel Narrow Band-Gap Copolymers Based on Pyridinthiadiazole for Semitransparent Organic Solar Cells. J. Phys. Chem. C 128, 1893–1900 (2024).
79. Lu, H. et al. Chlorinated Thiazole-Based Low-Cost Polymer Donors for High Efficiency Binary and Ternary Organic Solar Cells. CCS Chemistry 0, 1–10 (2023).
80. Zhang, L., Zhang, Z., Liang, H., Guo, X. & Zhang, M. A Non-Halogenated Polymer Donor Based on Imide Unit for Organic Solar Cells with Efficiency Nearly 16%. Chinese Journal of Chemistry 41, 2095–2102 (2023).
81. Kong, Y. et al. Semicrystalline Unfused Polymer Donors with Backbone Halogenation toward Cost-Effective Organic Solar Cells†. Chinese Journal of Chemistry n/a,.
82. Ha, J.-W., Park, B., Ko, S.-J. & Hwang, D.-H. Highly crystalline polycyclic aromatic lactam-based regioregular wide-band gap polymer donors for organic solar cells. J. Mater. Chem. C 12, 80–87 (2023).
83. Su, M. et al. Manipulating the Alkyl Chains of Naphthodithiophene Imide-Based Polymers to Concurrently Boost the Efficiency and Stability of Organic Solar Cells. ACS Appl. Mater. Interfaces 15, 37371–37380 (2023).
84. Hu, K. et al. Flexible side-chain optimization in polymer donor enables improved photovoltaic performance. Organic Electronics 116, 106765 (2023).
85. Zheng, J. et al. Effect of diazine isomers on photovoltaic properties of simple and efficient wide band gap polymer donor materials. Organic Electronics 125, 106964 (2024).
86. Zhang, M. et al. Side Chain Engineering of Two-Dimensional Polymeric Donors for High-Efficiency Organic Solar Cells. Energy Fuels 37, 6122–6128 (2023).
87. Pu, M. et al. Chlorination and Position Isomerization to Enhance the Photovoltaic Performance of Polymer Donors. Macromolecules 56, 5865–5872 (2023).
88. Yamanaka, K. et al. Interplay Between π-Conjugated Polymer Donors and Acceptors Determines Crystalline Order of Their Blends and Photovoltaic Performance. Advanced Energy Materials 13, 2203443 (2023).
89. Shen, S., Tu, Q., Tao, H., Ma, Y. & Zheng, Q. Side-chain engineering of wide-bandgap copolymers based on two different electron-deficient units for high-performance polymer solar cells. Polym. Chem. 14, 4227–4234 (2023).

90. Sato, N., Hwang, S., Tsuchii, Y. & Yasuda, T. Fused polycyclic lactam-based π-conjugated polymers for efficient nonfullerene organic solar cells. J. Mater. Chem. A 11, 9840–9845 (2023).
91. Tang, H. et al. Dithienobenzoselenadiazole-Based Polymer Donors with Tuned Side Chains for Efficient Polymer Solar Cells. ACS Appl. Energy Mater. 6, 4079–4088 (2023).
92. Weng, F. et al. Fluorination strategy on π-bridge of polymer donor for efficient photovoltaic performance. Journal of Power Sources 580, 233331 (2023).
93. Chen, J. et al. A Multifluorination Strategy Toward Wide Bandgap Polymers for Highly Efficient Organic Solar Cells. Angewandte Chemie International Edition 62, e202215930 (2023).
94. Xu, L.-Y. et al. A facile synthetic approach based on thieno[3,4-c]pyrrole-4,6-dione to construct polymer donors for highly efficient organic solar cells. Energy Environ. Sci. 16, 3942–3950 (2023).
95. Gao, Y. et al. Asymmetric Π-Bridge Engineering Enables High-Permittivity Benzo[1,2-B:4,5-b′]Difuran-Conjugated Polymer for Efficient Organic Solar Cells. Advanced Materials n/a, 2306373.
96. Liao, J. et al. Enhanced efficiency of polymer solar cells via simple fluorination on the π-bridge of polymer donors. Organic Electronics 108, 106611 (2022).
97. Jiang, Q. et al. Reducing steric hindrance around electronegative atom in polymer simultaneously enhanced efficiency and stability of organic solar cells. Nano Energy 101, 107611 (2022).
98. Shao, Y., Gao, Y., Sun, R., Zhang, M. & Min, J. A Versatile and Low-Cost Polymer Donor Based on 4-Chlorothiazole for Highly Efficient Polymer Solar Cells. Advanced Materials 35, 2208750 (2023).
99. Deng, J. et al. Layer-by-layer and non-halogenated solvent processing of benzodithiophene-free simple polymer donors for organic solar cells. Chemical Engineering Journal 443, 136515 (2022).
100. Liao, J. et al. Fluorine-Substituted π-Bridge through a Simple Method for Efficient Polymer Donor. Solar RRL 6, 2200697 (2022).
101. Keshtov, M. L. et al. New wide band gap π-conjugated copolymers based on anthra[1,2-b: 4,3-b': 6,7-c''] trithiophene-8,12-dione for high performance non-fullerene polymer solar cells with an efficiency of 15.07 %. Polymer 251, 124892 (2022).
102. Kini, G. P. et al. Tailoring Microstructure and Morphology via Sequential Fluorination to Enhance the Photovoltaic Performance of Low-Cost Polymer Donors for Organic Solar Cells. Macromolecular Rapid Communications 43, 2200070 (2022).
103. Ou, Z. et al. Engineering of the alkyl chain branching point on a lactone polymer donor yields 17.81% efficiency. J. Mater. Chem. A 10, 3314–3320 (2022).
104. Nakao, N. et al. Pronounced Backbone Coplanarization by π-Extension in a Sterically Hindered Conjugated Polymer System Leads to Higher Photovoltaic Performance in Non-Fullerene Solar Cells. ACS Appl. Mater. Interfaces 13, 56420–56429 (2021).
105. Liu, W. et al. Design of Near-Infrared Nonfullerene Acceptor with Ultralow Nonradiative Voltage Loss for High-Performance Semitransparent Ternary Organic Solar Cells. Angewandte Chemie International Edition n/a, e202116111.
106. Li, D.-X. et al. Quinoxaline-based Polymers with Asymmetric Aromatic Side Chain Enables 16.27% Efficiency for Organic Solar Cells. Chin J Polym Sci 41, 1002–1010 (2023).